

# Effect of CuO Nanoparticles on Performance and Emissions Behaviors of CI Engine Fueled with Biodiesel-Diesel Fuel Blends

Medhat Elkelawy<sup>1</sup>, El Shenawy A. El Shenawy<sup>1</sup>, Hagar Alm-Eldin Bastawissi<sup>2</sup>, and I. Abd-Elhay Elshennawy<sup>3</sup>

<sup>1</sup> Mechanical Power Engineering Dep., Faculty of Engineering, Tanta University, Tanta, Egypt – email: [medhatelkelawy@f-eng.tanta.edu.eg](mailto:medhatelkelawy@f-eng.tanta.edu.eg)

<sup>2</sup> Mechanical Power Engineering Dep., Faculty of Engineering, Tanta University, Tanta, Egypt

<sup>3</sup> Captain, Egyptian Army, Air Forces: [engibraheemshennawy@gmail.com](mailto:engibraheemshennawy@gmail.com)

**Abstract-** Recently the world has a very important need for replacement fossil fuel with renewable sources of energy. Greenhouse effect is considered one of bad effects of fossil fuels, which causes increase of global temperature. Biodiesel is one of fossil fuel alternatives, which can be produced from many organic sources. Scientists are searching for adding nano-materials to fueling system, which can modify fuel characteristic in compression chambers. In this study diesel fuel will be replaced with blends of diesel and biodiesel produced from waste cooking oil (WCO) is created using a catalytic transesterification reaction (CTR). With the addition of a low concentration of alcohol over the period of an hour at a reaction temperature of 65 °C, (CTR) converts (WCO) to methyl esters. Blends consisting of (40 % diesel, 60 % biodiesel and CuO nano-material with different concentration) will be prepared for fueling direct injection engine four-stroke. The engine will be run at 1400 rpm with natural aspiration under various loads. Using blends of (pure diesel, B40 [consist of 60 % biodiesel and 40 % diesel], 50B40 [consist of 60 % biodiesel, 40 % diesel and 50 mg CuO], 100B40 [consist of 60 % biodiesel, 40 % diesel and 100 mg CuO], 150 [consist of 60 % biodiesel, 40 % diesel and 150 mg CuO] and pure diesel). On engine performance and emissions, the impact of using copper oxide has been studied. The results of the experiment demonstrate that diesel engines can run on various mixtures of fuel, biodiesel, and CuO nano-material under the same operating conditions. The obtained data indicates that a 10% increase in brake thermal efficiency was noted, decrease in exhaust temperature with 11.6 % and decrease in brake specific fuel consumption with 6.66 %.

**Keyword:** internal combustion engine; emissions; biodiesel; nanoparticles; waste cooking oil; direct injection diesel engine

## I. INTRODUCTION

Recently, the searching for new and renewable sources of fuel has been increased [1-3]. Using sunflower and soyabean biodiesel with silver thiocyanate nano-material modify BTE [3-6]. This is after agreement of many countries and institutions for adopting the international trends to preserve the environment by reducing emissions and reducing fossil fuel consumption [1, 7]. So, they were working to raise the efficiency of combustion systems performance, especially in the application of internal combustion engines [8-11]. To achieve this goal, all research authorities sought to maximize the production of alternative fuels that can be used in internal combustion engines without fundamental change in the original fuel systems [12-14].

The production of biofuel from used edible oils, the cultivation and harvesting of algae [15, 16], and the fermentation of agricultural residues were among the most

important research directions in this regard [17]. In this context, the researchers worked through innovative mathematical and numerical methods in their research with the use of nanometric materials technologies to reach the best performance parameters in internal combustion engine systems [18-21]. Fossil fuels are considered a non-renewable energy source [22]. Fossil fuel price changes according to world political and economic problems and may be used as a mean of political pressure on any country [23, 24]. Emissions from fossil-fueled engine have a harmful environmental effect [25-27]. These emissions should be reduced to fit environmental guidelines. Scientists have been investigated in using nano-materials with biodiesel in direct injection engine [28-30]. The results show that nano-material with biodiesel has modified engine characteristics.

There are some of results, which had been approved [31, 32]. Using B25 with 50 ppm alumina nano-material, engine performance increased by 4.8 %, BSFC was decreased by 8.5 % and HC, CO and smoke concentrations were diminished by 36 %, 20 % and 44 %, respectively [33]. Using novel graphene oxide GO with waste cooking biodiesel with concentrations of 100 and 200 ppm leads to lesser WCB100GO and WSBD 200GO BSFC (3% and 7% kg/kWh). In spite decrease exhaust gas temperature by 7 % and 16 %, respectively and increase of BTE by 4 % and 1.2 %, respectively [34].

Using CeO<sub>2</sub> nano-material on neat palm oil methyl ester and diesel blends with concentration of 10, 20 and 30 nm reduces BSFC and increase BTE. However, CO and HC concentrations were reduced by 3.6 % and 4.2 %, respectively. NO<sub>x</sub> and smoke emissions reduced by using CeO<sub>2</sub> nano-material by 3.8 % and 6.4 %, respectively [35]. Adding 100ppm TiO<sub>2</sub> to Pongamia biodiesel fuel leads to reduce HC, smoke concentrations, NO<sub>x</sub> and CO by 2.1 %, 2.7 %, 3.8 % and 1.9 %, respectively [36]. Running diesel engine with WCO B20 using carbon nanotubes and graphene nano sheet with concentration of 100 ppm improved BTE by 8 % and 19 %, respectively. Causing a decrease of smoke by 28 % and 54 %, respectively, CO by 27 and 47 %, respectively, NO<sub>x</sub> by 22 % and 44 %, respectively [37].

Operating direct injection diesel engine at constant speed with natural aspiration with mahua biodiesel by adding 100 ppm copper oxide of 10 and 20 nm had improved BSFC and BTE by 1.3 and .7%, respectively [38]. Causing an improve in CO, NO<sub>x</sub>, HC, and smoke emission by 4.9, 3.9, 5.6, and 2.8%, respectively [39]. Using Sr@ZnO nano-material with 30, 60 and 90 ppm in blend 20 % Ricinus

communis biodiesel and 80% diesel in common rail direct injection engine at constant speed leads to increase in HRR, BTE and cylinder pressure increased by 24.35 %, 20.83 % and 9.55 %, respectively. Although ID, BSFC, smoke, CD, HC, CO and CO<sub>2</sub> reduced by 20.64 %, 20.07 %, 27.90 %, 14.5 %, 26.81 %, 47.63 % and 34.9%, respectively.

While NO<sub>x</sub> concentration had a slightly increase [40]. There is an improve in BSFC and BTE by using (CeO<sub>2</sub>) nano-material with biodiesel in DI engine and reduction in concentration of soot, NO<sub>x</sub>, smoke opacity, CO and HC [41]. Using a nanosized silver thiocyanate structure in diesel engine fueled by 50 % diesel and 50 % biodiesel improves engine performance and emissions [42]. Using 25, 50 and 75 nano-material of cerium coated zinc oxide (Ce-ZnO) with diesel-soybean biodiesel blends in diesel engine leads to BTE and HRR increasement by 20.66 % and 18.1 %, respectively. Causing reduction of CO, smoke, and HC by 30 %, 18.7 %, and 21.5 %, respectively [43]. There is a noticeable increase of BTE by 27.16 % by using 50 % diesel and biodiesel with adding 200 ppm silver thiocyanate AgSCN and 4% hydrogen peroxide (H<sub>2</sub>O<sub>2</sub>) [44].

Using (SC1) [Mn (EIN)<sub>4</sub>(NCS)<sub>2</sub>] 12.25 nm nano-material with concentration of 50, 100 and 150 in diesel engine fueled by 49 % biodiesel and 49% diesel and 2% hydrogen peroxide (H<sub>2</sub>O<sub>2</sub>) leads to improve BTE by 14.8–20.52%. Causing reduction in smoke, CO and HC by 32–44.27 %, 48.19–62.05 % and 15.34–60.94 % comparing with pure diesel [45]. Operating diesel engine with natural aspiration by adding 77 nm CuO with concentration of 1000 and 2000 ppm caused to reduce emissions rates as CO reduced by 14.6 % and 20.8 %, HC reduced by 6.2 % and 13.4 %, and NO<sub>x</sub> by 4 %, and 4.7 %. Both concentrations of CuO enhance the heating value of the diesel fuel. (BSFC) decreased by 4.5 % and 8 % while (BTE) increased by 5.5 % and 14.6 % for 1000-CuO and 2000-CuO, respectively [46].

Adding (CeO<sub>2</sub>) nano-material of 25, 50, 75 and 100 ppm to diesel engine fueled by biodiesel blends improves the BTE, reduces emissions and BSFC [47]. Running diesel engine with adding TiO<sub>2</sub> metal-based material increases the maximum cylinder pressure HRR, as improvement the engine performance and combustion [48]. Adding TiO<sub>2</sub> to diesel engine increase in heating value and Cetane number [49]. Adding graphene oxide (GO) nano-material to diesel engine fueled by biodiesel blends causes a reduction in CO, UHCs and BSFC, although there is an increase in NO<sub>x</sub> concentration [50]. Running diesel engine with biodiesel blends by adding carbon coated aluminum (Al@C) nano-material causes a reduction in BSFC, CO, NO<sub>x</sub> concentrations [51]. Therefore, engineers, scientists and researchers are looking for suitable replacement for diesel which can be used in direct injection diesel engines.

In this case, WCO is produced by Catalytic transesterification reaction. After producing biodiesel process washing process takes place to get out of any impurities and modify biodiesel properties such as density and viscosity. Different percentages blends will be made with diesel, biodiesel, and CuO nano-material. The diesel engine will run with varied loads at a constant speed of 1400 rpm. The engine is connected to a hydraulic dynamometer, which allows the operator to switch loads. The impact of

using different blends will be compared with diesel characteristics by measuring brake specific fuel consumption BSFC, brake thermal efficiency BTE, exhaust temperature Tex, and emissions rate.

## II. EXPERIMENTAL SETUP AND PROCEDURE

### A. Engine and Test Rig Installation

The test rig has a diesel engine model (ZS1125NM) attached to hydraulic dynamometer type (ATE-160 LC)[4, 52]. The dynamometer enables the operator to change loads during operating the engine. Flow control valves are attached to the test rig, which was created to allow the operator to choose and change the fuel type while the engine was operating. For fuel consumption, the test rig has grades on fueling system, which enables the operator to calculate the amount of fuel consumed in certain time[53]. Gas analyzer device model (GASBOARD-5020) is attached to test rig, which measures emissions (CO, CO<sub>2</sub>, O<sub>2</sub>, UNHC, NO<sub>x</sub>). Soot analyzer device model (GASBOARD-6010) is used which measures soot rate in exhaust gases[54]. RPM indicator is used to engine speed. Thermocouples are applied to measure the temperatures of cooling water, oil, and inlet / exhaust. The schematic and actual test rig is shown in figures 1 and 2.

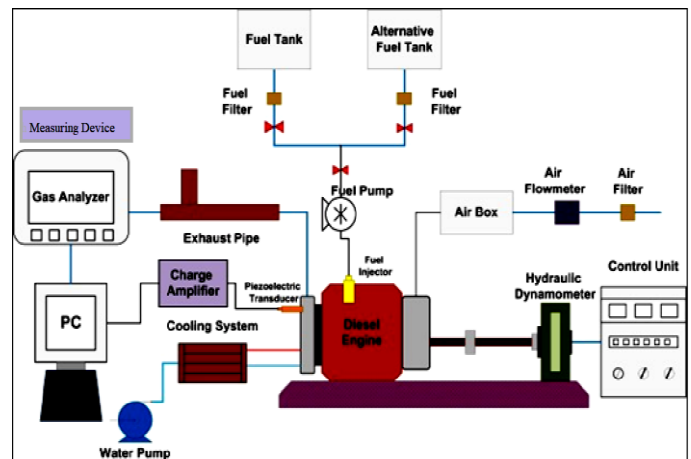


Figure 1. Schematic diagram of test rig

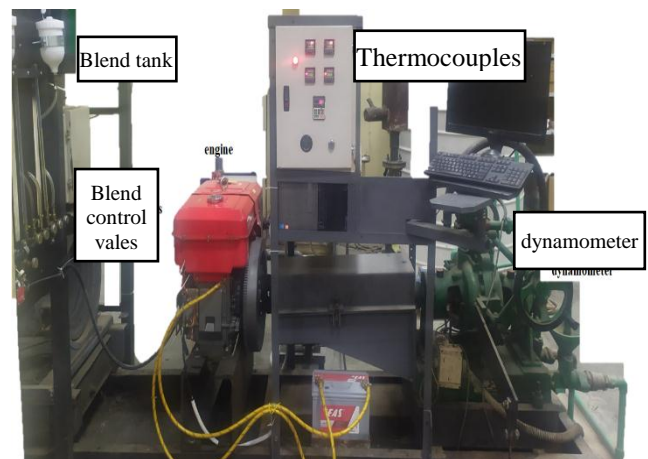


Figure 2. Actual photo of the test rig

### B. Engine and dynamometer Specifications

The characteristic of direct injection diesel engine is illustrated in table 1. Hydraulic dynamometer model (ATE-160 LC) load cell with digital torque indication attached to engine. Load cell capacity ranges from 0 to 350 kg (0 to 1050 N-m)[55]. Lever arm calibration length[56, 57]: 0.7645 m. wheel and sensor with 60 teeth. shaft-mounted half of the coupling. Hydraulic and water absorption.

### C. Nano particle properties

Due of its distinctive qualities, including improved electrical conductivity, hardness, and ductility, nanomaterial research is garnering more and more attention [58]. Metals and alloys' increased hardness and strength, semiconductors' improved luminescence, ceramics' formability, and their use in magnetic storage media are all contributing factors. transformation of solar energy, electronics, and catalysis [58]. One of the most important the oxides of transition metals is copper oxide. Copper oxide plays a crucial role in the production of high-*tc* superconductors, photoconductive and photothermal applications [59]. Copper oxide nano-material were synthesized via the sono-chemical method [60]. Sol-gel technique [61] at room temperature, one-step solid state reaction technique [62], electrochemical method [63], and co-implantation of metal and oxygen ions [64].

Copper oxide size and shape was obtained by using TEM has been on JEOL JEM-2100 accelerating voltage of 200 kV, and a high-resolution transmission electron microscope, respectively. At a 200kV accelerating voltage, wide-angle X-ray diffraction and small-angle capability XRD experiments were conducted, respectively. An XRD pattern has been performed within a range of 2 theta (20-80), with minimum step size 2Theta:0.001, and at wavelength ( $\lambda$ ) = 1.54614.

**Table 1. Direct injection diesel engine specification.**

Parameters	Specifications
Type of engine	Model number model ZS1125NM horizontal, single cylinder, four strokes, water cooling
Bore* stroke* swept volume	125 mm * 120 mm* 1.473 L
Power	9 HP /2200 rpm
Injection pressure	20±0.49 MPa
Cooling system	Condenser
Lubrication system	Pressure /splash

**Table 2. Vopper oxide nano-material specification**

Parameters	Specifications
Appearance (Color)	Dark Brown
Appearance (Form)	powder
Manufacture date	5/2017
Expire date	8/2023
Solubility	Suspended in
Average Size (TEM)	Water40 ± 5nm

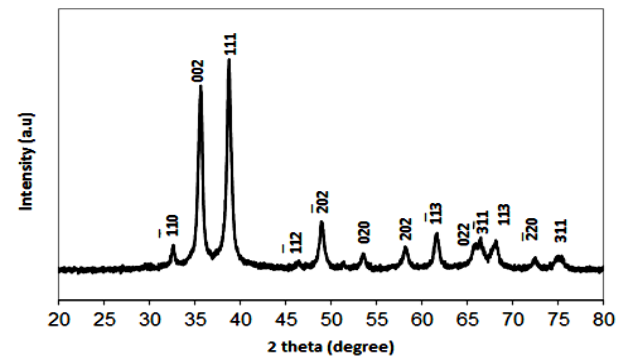


**Figure 3. XRD pattern**

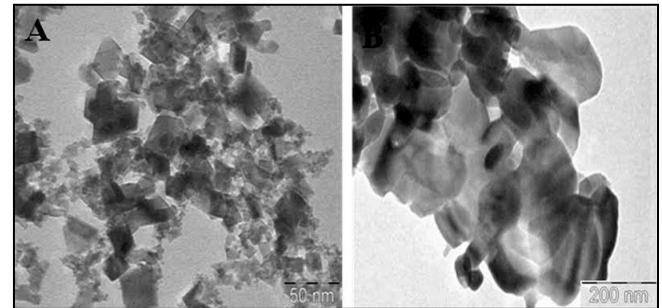


**Figure 4. TEM micrographs properties:**

### D. Production of Biodiesel

In production process, WCO is converted into biodiesel by a catalytic transesterification mechanism. Catalyst (NaOH), methanol, and used waste cooking oil are the reaction's components. The reaction needs 60 minutes with mixing conditions at 65 °C. The oil will be burnt if reaction temperature becomes more than 65 °C therefore, the reaction must be under thermal control. The electric mixer is programmed to operate until the reaction temperature reaches 65 °C. If reaction temperature rises, the mixer will be turned off. At a volumetric oil to methanol ratio of 1:1.2035 and a catalyst weight concentration of.65%, the highest biodiesel production yield of 93% is achieved. The reaction produces glycerol, biodiesel, fat, and dirt. For a good separation, glycerol needs to be separated for roughly 12 hours. Figures 5 and 6 depict the production bench and production rig schematic diagram.

Biodiesel washing process was performed after biodiesel production process washing process takes place. Biodiesel must be cleaned of fats and other impurities using a washing procedure. With a volumetric ratio of 1:1, hot water is employed at 100 °C. Washing process needs a special technique for avoiding foaming of biodiesel so washing mixer cannot run continuously. The mixer is controlled to run for 5 seconds and stop for 3 seconds in each washing process. After 1 minute, biodiesel and water need time to be separated from each other. Repeating this process about 3:5 times for ensuring good washing. Biodiesel may turn into soap if washing process takes long time more than 1 minute. Biodiesel physical properties change during washing like density and color. The decrease in density is benefit for fueling system. By the end of washing process, the biodiesel is ready for using in diesel engine. For storing biodiesel, it is crucial to



maintain it in sealed containers away from air to prevent oxidation.

Comparison between diesel and biodiesel were performed after production of biodiesel should have physical and thermal characteristic as diesel to ensure suitable replacement for diesel in fueling system and combustion chamber. The same fueling system that was made to use diesel fuel should be used for biodiesel. Large difference in any characteristic between biodiesel and diesel leads to certain problem in feeding, combustion chamber and exhaust gas analysis. Table 3 shows the characteristic variation between diesel and biodiesel.

Table 3. Biodiesel and diesel characteristics comparison

Fuel type	Diesel	biodiesel	Standards
Density (kg/m <sup>3</sup> )	780:860	850:900	ASTMD 1298
Heating value (MJ/kg)	HHV=47	HHV=40	ASTMD 240
Kinematic viscosity (mm <sup>2</sup> /s)	3.68	5.3	ASTMD 445
Flash point (°C)	58	167	ASTM D93
Cetane no	54	62	ASTMD 613

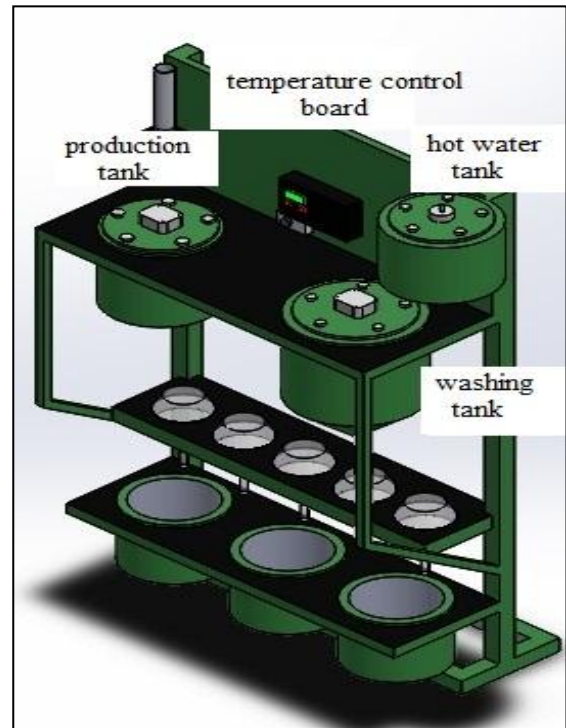


Figure 5. Actual Production bench

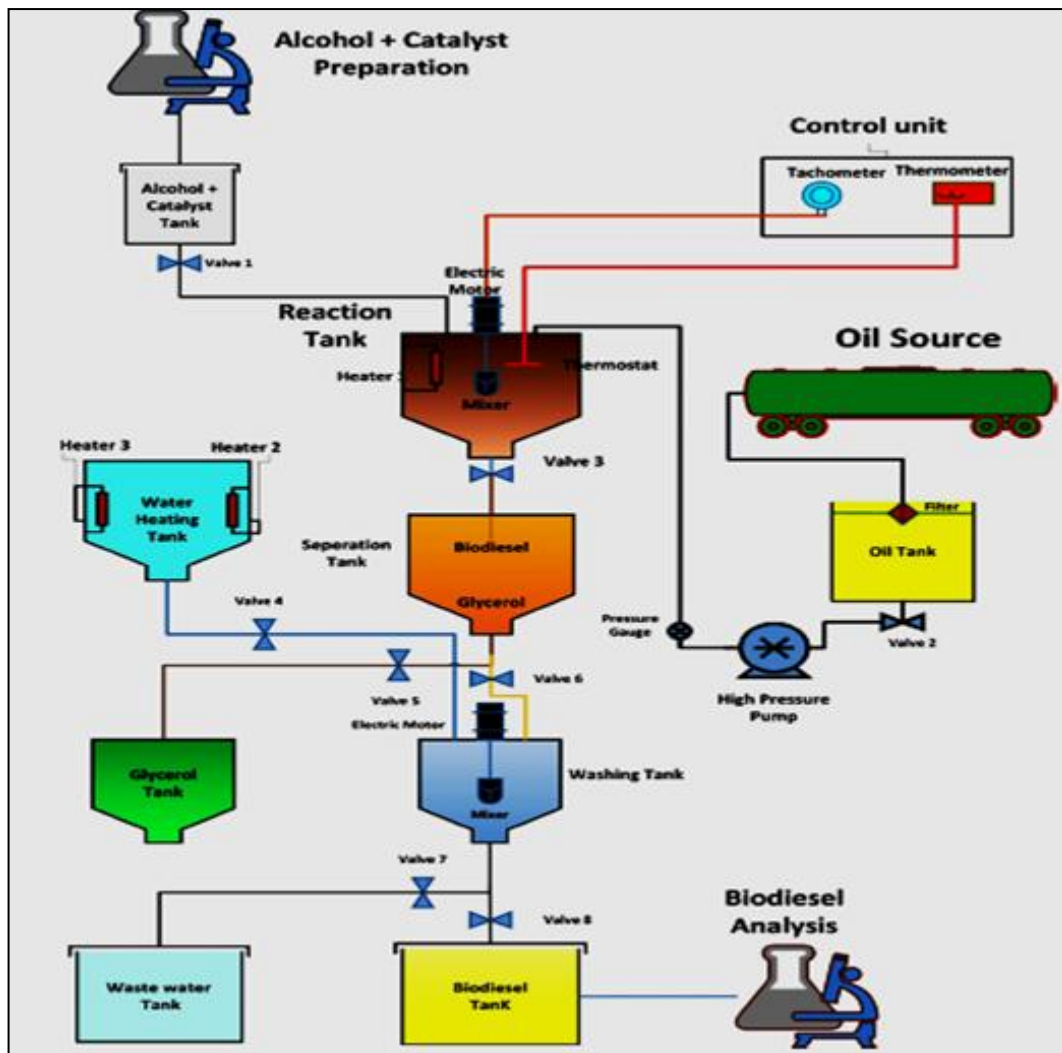


Figure 6. Schematic diagram of production rig

It is clear from the table that the heating value of biodiesel is slightly lower than that of diesel. In biodiesel blends, this drop will result in an increase in the specific fuel consumption. Biodiesel has large kinematic viscosity than diesel that will cause a difficulty in fuel flow through the fueling system. Biodiesel has large density than diesel that will lead to poor vaporization in combustion chamber. However, biodiesel has a greater cetane number than diesel, which will improve explosion postponement period.

Mixing Process was performed to get homogenous mixing between biodiesel and diesel. Diesel and biodiesel were added by desirable percentage in mixing container supplied with mixing motor. Mixing time may take one hour to ensure good mixing. Poor mixing leads to density separation. Adding nano-material to the fuel blend needs a professional skill. Homogenous distribution of nanomaterial in blend is desired. The name of the blend should reflect all composition of it. For example, D60 B40 N 100 means (60 % pure diesel +40 biodiesel +100 mg nanomaterial/liter). After mixing process the blend is ready to use in engine to be tested.

Running Process for the engine was achieved after mixing process, running process takes place. It is necessary to start the engine up with diesel and run it for a little while first. Fueling system control valves is used to switch between blends. After turning fueling system to blend, the operator should wait a short of time to let the blend get into fueling system. The operator should let the new blend time for getting into fueling lines and fuel filter. Before measuring process, the operator should wait several minutes to let the engine to reach steady state point.

Measuring process takes place after reaching steady state condition. Thermocouples (k-type) are used in air inlet and exhaust gas to measure inlet air and exhaust gas temperature. Graded glass tubes are fixed on fueling control board which enable the operator to measure fuel consumption. The operator can change loads while the engine is operating thanks to a hydraulic dynamometer that is linked to the engine. Load cell is connected to dynamometer to print out the load at digital screen. Gas analyzer and soot analyzer device are used to measure emission rates (CO, CO<sub>2</sub>, O<sub>2</sub>, UNHC, and NO<sub>x</sub>).

Error Analysis of the used thermocouples and gas analyzer are attached to test rig. Which have range, uncertainty and accuracy. Some physical characteristics of the engine have a significant impact on the empirical results, which could lead to inaccurate data. Therefore, mathematical calculations have been made to ensure the precision and accuracy of the experimental results. Equation 1 illustrates the engine's operational parameters and emissions uncertainty calculations.

$$W_R = \left( \left( \frac{\partial R}{\partial x_1} w_1 \right)^2 + \left( \frac{\partial R}{\partial x_2} w_2 \right)^2 + \dots + \left( \frac{\partial R}{\partial x_n} w_n \right)^2 \right)^{\frac{1}{2}} \quad (1)$$

$W_R$  reflects the overall amount of uncertainty for the observed data under test.  $w_1, \dots, w_2, \dots, w_n$  are engine parameters uncertainty values. Where R is the main

function for  $X_1, X_2, \dots, x_n$  as the engine measured parameters. Engine execution parameters like BSFC, BTE, speed, and break power had uncertainty values of  $\pm 1.5\%$ ,  $\pm 1\%$ ,  $\pm 0.3\%$ , and  $\pm 0.5\%$ , respectively. Additionally, the engine emissions uncertainty value was within the permitted limit of  $\pm 0.25\%$ , where  $\pm 0.15\%$ ,  $\pm 1.1\%$ , and  $\pm 0.65\%$  were the uncertainty values of the K-type thermocouples, airflow rate, and fuel flow rate, respectively. Table 4 illustrates the uncertainties of gas analyzer.

Table 4. Uncertainties of gas analyzer device

Parameters	Range	Accuracy	Uncertainties (%)
Tex	0:1000 °C	$\pm 1$ oC	$\pm 0.1$
CO	0:15.0 vol %	$\pm 0.01$ vol %	$\pm 0.07$
CO <sub>2</sub>	0:20.0 vol %	$\pm 0.01$ vol %	$\pm 0.05$
O <sub>2</sub>	0:25.0 vol %	$\pm 0.01$ vol %	$\pm 0.04$
HC	0:30000 ppm vol.	$\pm 1$ ppm vol.	$\pm 0.003$
NO <sub>x</sub>	0:1000 ppm vol.	$\pm 1$ ppm vol.	$\pm 0.1$
Speed	0:8000 rpm	$\pm 5$ rpm	$\pm 0.06$
Torque	0:110 Nm	$\pm 0.05$ Nm	$\pm 0.05$
Power	0:92 kW	$\pm 0.07$ kW	$\pm 0.08$
Flow rate	0.1:30 l/h	$\pm 0.02$ l/h	$\pm 0.06$
SFC	–	–	$\pm 0.4$
LHV	–	–	$\pm 0.1$
BTE	–	–	$\pm 0.2$
Kinematic Viscosity	0.2:20000 mm <sup>2</sup> /s	–	$\pm 0.1$
Dynamic Viscosity	0.2:20000 mPa.s	–	$\pm 0.1$
Density	0.65:3.0 g/cm <sup>3</sup>	0.0001g/cm <sup>3</sup>	$\pm 0.003$
Humidity	3:99%	$\pm 0.5\%$	$\pm 0.5$
Temperatures	0:1000 o C	$\pm 1$ o C	$\pm 0.1$
Ambient pressure	700:1100 mbar	$\pm 1$ mbar	$\pm 0.09$

Table 5. The list of tested conditions:

Case	Symbol	Composition
1	D100 B0 N00	100 % pure diesel
2	D60 B40 N00	60 % pure diesel +40 biodiesel
3	D60 B40 N50	60 % pure diesel +40 biodiesel +50 mg nanomaterial/liter
4	D60 B40 N100	60 % pure diesel +40 biodiesel +100 mg nanomaterial/liter
5	D60 B40 N150	60 % pure diesel +40 biodiesel +150 mg nanomaterial/liter

### III. RESULTS AND DISCUSSIONS

For each running case, different data are obtained after the engine has been run with various blends and measurement methods.

#### A. Impact of using copper oxide on brake specific fuel consumption

BSFC is among the most important parameters of engine performance. It is defined as the ratio of produced power in the engine to fuel consumption at specific time. From figure 7 it is clear that the BSFC goes down by elevating load. By comparing diesel with D60 B40 N00 it is shown that pure diesel BSFC at any load is smaller than D60 B40 N00 BSFC due to biodiesel's high viscosity and low heating value. Biodiesel high viscosity leads to poor vaporization in combustion chamber that will lead to consume more fuel than pure diesel at the same load. Biodiesel low heating value than diesel causes an increase in fuel consumption.

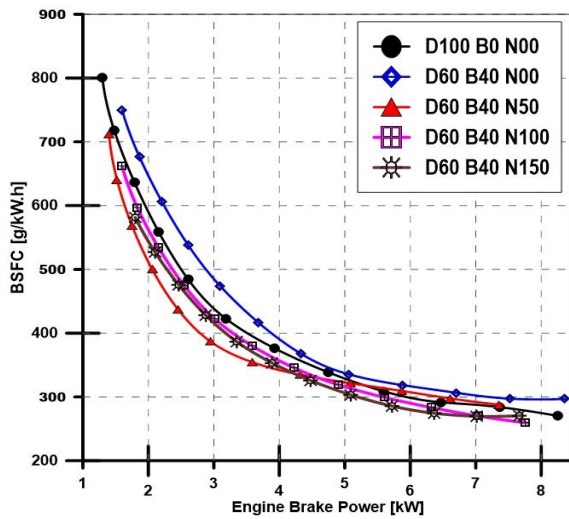


Figure 7. Brake specific fuel consumption

By adding CuO nanomaterial BSFC starts to decrease until it be smaller than pure diesel BSFC. The decrease of BSFC increase by increasing CuO nanomaterial. The maximum decrease in BSFC is between pure diesel and D60 B40 N150 is 6.66 % at 6 kW. This decrease makes CuO nanomaterial one of the best choices to be used with biodiesel blends to replace diesel in direct injection engines.

#### B. Impact of using copper oxide on engine brake thermal efficiency

BTE is regarded as one of the most crucial engine characteristics since it measures the amount of energy that is converted from fuel into power. Figure 8 of the BTE diagram shows that the BTE rises as the load rises because of complete combustion. By comparing pure diesel BTE with D60 B40 N00 it is shown that D60 B40 N00 BTE is smaller than pure diesel because of low heating value. By adding CuO nano, material BTE starts to increase gradually until it exceeds pure diesel BTE reaching its maximum value at D60 B40 N150. The maximum BTE increase is 10 % at 6 kW is. This increase in BTE shows that by adding CuO nanomaterial the BTE will be modified.

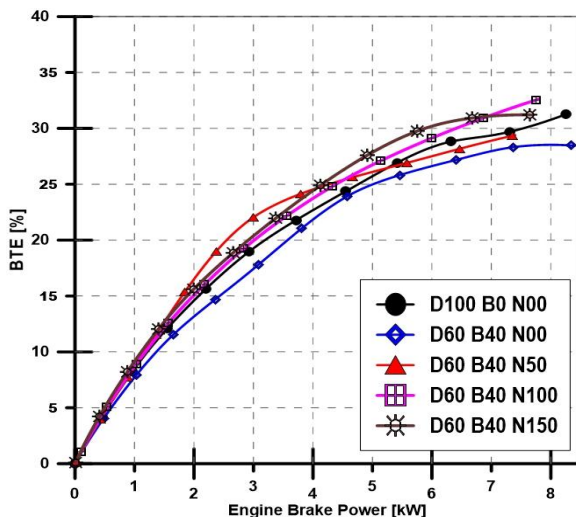


Figure 8. Engine brake thermal efficiency

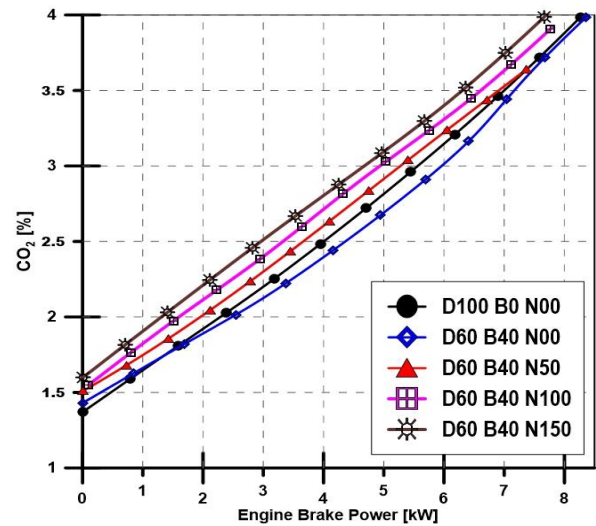


Figure 9. Carbon dioxide rate

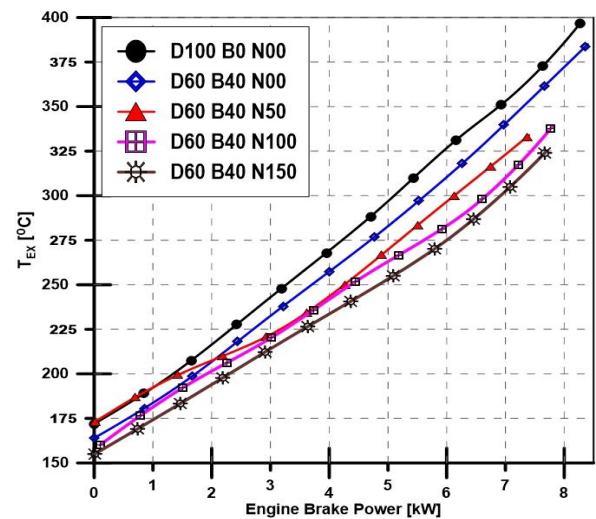


Figure 10. Exhaust temperature

#### C. Impact of using copper oxide on carbon dioxide rate

Carbon dioxide concentration refers to complete combustion possibility. Figure 9 shows CO<sub>2</sub> concentration for all blends. The figure shows that by increasing the load CO<sub>2</sub> concentration increase due to the increase of combustion reaction rate. By comparing diesel with blends, it is clear that CO<sub>2</sub> concentration decreases by using D60 B40 N00, but it begins to increase by using CuO until it exceeds pure diesel value. The maximum increase between D60 B40 N150 and pure diesel is 11.1 % at 6 kW. By considering the increase in BTE and decrease of BSFC and CO<sub>2</sub> concentration by using CuO it is obvious that the more using CuO nanomaterials the more complete combustion takes place.

#### D. Impact of using copper oxide on engine exhaust temperature

Tex relates to the rate of combustion reaction in the combustion chamber. Figure 10 illustrates engine exhaust gases temperature for blends. It is evident from the diagram that when load increases, exhaust gas temperature rises as a result of an increase in combustion chamber fuel consumption. By comparing diesel Tex with blends, it has



shown that by using biodiesel exhaust temperature decrease than pure diesel. The more CuO used the more exhaust temperature decreases. The maximum decrease in Tex is between pure diesel and D60 B40 N150 is 18.4 % at 6 kW. This drop in exhaust temperature is encouraging because it lessens the engine's thermal stress.

#### E. Impact of using copper oxide on unburned hydrocarbon

A higher rate of unburned hydrocarbons in exhaust gases indicates incomplete combustion inside the combustion chamber. From figure 11 it is obvious that hydrocarbons decrease by increasing load because BTE increases and CO<sub>2</sub> concentration increases with increasing load. By comparing UBHC rates in diesel and blends it is obvious that by using biodiesel and adding CuO nano-material the UBHC decreases. The maximum decrease in UBHC is between pure diesel and D60 B40 N150 is 75 % at 6 kW. This decrease refers to the efficiency of combustion which tips the balance of using CuO with biodiesel in compression ignition engines.

#### F. Impact of using copper oxide on nitrogen oxide rate

Figure 12 illustrates different concentrations of NO<sub>x</sub> on exhaust temperature. There are a lot of factors which effect on nitrogen oxide rate such as high reaction temperature which named thermal NO<sub>x</sub>, residence time, availability of nitrogen and oxygen percentage in fuel. From NO<sub>x</sub> diagram, it is clear that concentration of NO<sub>x</sub> in exhaust gas increases by increasing load because of high reaction temperature. From the figure, it is shown that NO<sub>x</sub> concentration decreases by using CuO nano-material directly. This decrease due to decreasing exhaust temperature by using CuO. NO<sub>x</sub> decrease is considered one of the most parameters that encourage using CuO nano-material in diesel engine. The maximum decrease in NO<sub>x</sub> is between pure diesel and D60 B40 N150 is 20 % at 6 kW.

#### G. Impact of using copper oxide on carbon monoxide rate

Figure 13 shows the concentration of CO in exhaust gases. CO percentage in exhaust gases reflects incomplete combustion rate. Poor air/fuel ratios and fuel evaporation lead to incomplete combustion. From CO graph it is clear that CO concentration increase with increasing load, but with comparing diesel with blends it is obvious that CO concentration decreases by increasing CuO in blends. The maximum decrease in CO concentration is between pure diesel and D60 B40 N150 is 19 % at 6 kW. By decreasing of both CO and UNHC concentration, it is clear that complete combustion is highly related with CuO percentage as it increases by increasing CuO in blends.

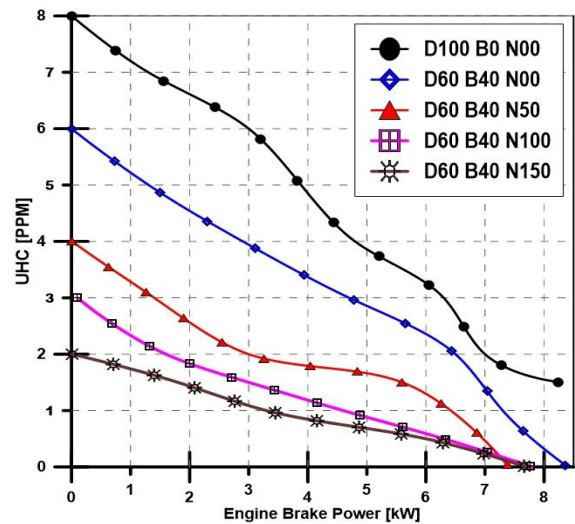


Figure 11. Unburned hydrocarbon

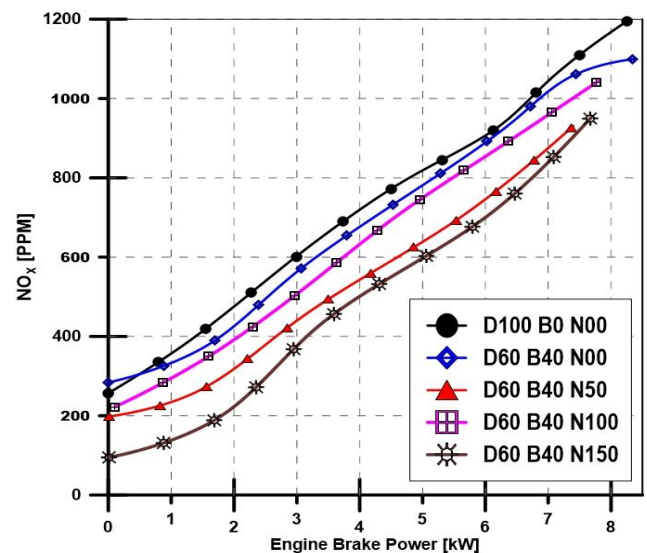


Figure 12. Nitrogen oxide rate

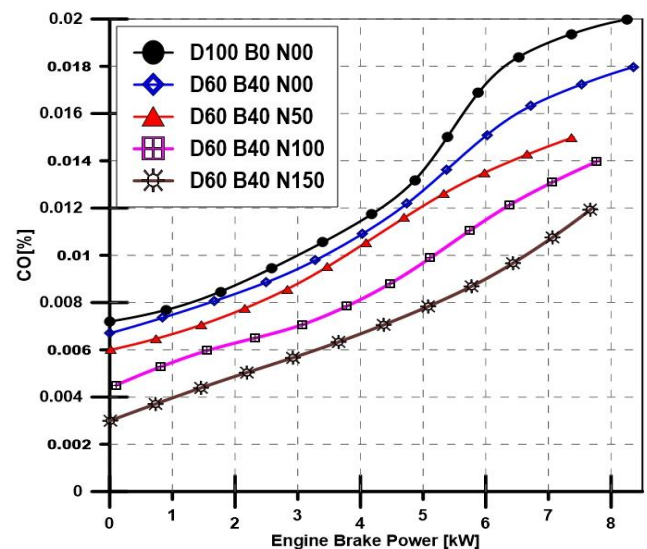


Figure 13. Carbon monoxide rate

## IV. CONCLUSION

By catalytic transesterification reaction, 93% of the WCO was converted into biodiesel. Reaction conditions are 65 °C reaction temperature, .2035:1 methanol to WCO volumetric ratio .65 % weight concentration of catalyst and 60 minutes reaction time. The cost and production process for biodiesel are extremely straightforward. The properties of the produced biodiesel are equivalent to those of pure diesel. It is relatively easy to operate direct injection engines with mixtures of diesel, biodiesel, and CuO nano-material. The following results have been acquired after running the engine with various blends without making any modifications to the engine and examining the data of loads, fuel consumption, and exhaust composition.

- Brake thermal efficiency increases with using copper oxide with 10 %.
- CO<sub>2</sub> concentration increases with using copper oxide with 11.1%.
- CO and UBHC concentration decrease by using copper oxide by 19 % and 75 % representatively.
- Exhaust temperature decreases with using copper oxide with 18.4 %.
- BSFC decreases with using copper oxide with approximate ratio of 6.66%.
- NO<sub>x</sub> concentration increases with using copper oxide with 20 %.

Finally, the diesel engine can operate with various diesel, biodiesel, and copper oxide blends under the same operating circumstances without requiring any engine modifications.

## ACKNOWLEDGMENTS

The authors gratefully acknowledge the Tanta University Research Fund's financial support. The Tanta University Research Fund supported this experimental investigation with a research grant. (Code: tu: 02-19-01).

**Funding:** This research has not received any type of funding.

**Conflicts of Interest:** The authors declare that there is no conflict of interest.

## ABBREVIATIONS

WCO	Waste Cooking Oil
WCBD	Waste Cooking Biodiesel
CTR	Catalytic Transesterification Reaction
CuO	Copper Oxide
GO	Graphite Oxide
CeO <sub>2</sub>	Cerium Oxide
HC	Hydrocarbon
NO <sub>x</sub>	Nitrogen Oxide
Ce-ZnO	Cerium Doped Zinc Oxide
Sr@ZnO	Cerium Coated Zinc Oxide
Al@C	Carbon Coated Aluminum
H <sub>2</sub> O <sub>2</sub>	Hydrogen Peroxide
CO	Carbon Monoxide
CO <sub>2</sub>	Dioxide
O <sub>2</sub>	Oxygen
UNHC	Unburned Hydrocarbon

TiO <sub>2</sub>	Titanium Dioxide
NaOH	Sodium Hydroxide
PPM	Part Per Million
BTE	Brake Thermal Efficiency
BSFC	Brake Specific Fuel Consumption
HRR	Heat Release Rate
HP	Horsepower
XRD	X-Ray Powder Diffraction
TEM	Transmission Electron Microscopy
rpm	Revolution Per Minute
ID	Ignition Delay
CD	Combustion Duration
Mn	Manganese
HHV	Heigh Heating Value
ASTMD	Appearance Smell Taste Mouthfeel Drinkability
PPM	Part Per Million
VOL	Volume

## REFERENCES

- [1] M. Elkelawy, Z. Yu-Sheng, H. A. El-Din, and Y. Jing-zhou, "A comprehensive modeling study of natural gas (HCCI) engine combustion enhancement by using hydrogen addition," SAE Technical Paper 0148-7191, 2008.
- [2] A. Singh, S. Sinha, A. K. Choudhary, H. Panchal, M. Elkelawy, and K. K. Sadasivuni, "Optimization of performance and emission characteristics of CI engine fueled with Jatropa biodiesel produced using a heterogeneous catalyst (CaO)," *Fuel*, vol. 280, p. 118611, 2020/11/15/ 2020.
- [3] E. A. El Shenawy, M. Elkelawy, H. A.-E. Bastawissi, H. Panchal, and M. M. Shams, "Comparative study of the combustion, performance, and emission characteristics of a direct injection diesel engine with a partially premixed lean charge compression ignition diesel engines," *Fuel*, vol. 249, pp. 277-285, 2019/08/01/ 2019.
- [4] M. Elkelawy, E. A. El Shenawy, S. k. A. Almonem, M. H. Nasef, H. Panchal, H. A.-E. Bastawissi, *et al.*, "Experimental study on combustion, performance, and emission behaviours of diesel /WCO biodiesel/Cyclohexane blends in DI-CI engine," *Process Safety and Environmental Protection*, vol. 149, pp. 684-697, 2021/05/01/ 2021.
- [5] E. A. El Shenawy, M. Elkelawy, H. A.-E. Bastawissi, M. M. Shams, H. Panchal, K. Sadasivuni, *et al.*, "Investigation and performance analysis of water-diesel emulsion for improvement of performance and emission characteristics of partially premixed charge compression ignition (PPCCI) diesel engines," *Sustainable Energy Technologies and Assessments*, vol. 36, p. 100546, 2019/12/01/ 2019.
- [6] M. Elkelawy, H. Alm-Eldin Bastawissi, E. A. El Shenawy, M. Taha, H. Panchal, and K. K. Sadasivuni, "Study of performance, combustion, and emissions parameters of DI-diesel engine fueled with algae biodiesel/diesel/n-pentane blends," *Energy Conversion and Management: X*, vol. 10, p. 100058, 2021/06/01/ 2021.
- [7] M. Elkelawy, E. El Shenawy, S. khalaf Abd Almonem, M. Nasef, H. Panchal, H. A.-E. Bastawissi, *et al.*, "Experimental study on combustion, performance, and emission behaviours of diesel/WCO biodiesel/Cyclohexane blends in DI-CI engine," vol. 149, pp. 684-697, 2021.
- [8] M. Elkelawy, S. E.-d. H. Etaiw, H. A.-E. Bastawissi, H. Marie, A. M. Radwan, M. M. Dawood, *et al.*, "WCO biodiesel production by heterogeneous catalyst and using cadmium (II)-based supramolecular coordination polymer additives to improve diesel/biodiesel fueled engine performance and emissions," vol. 147, pp. 6375-6391, 2022.
- [9] S. C. Sekhar, K. Karuppasamy, R. Sathyamurthy, M. Elkelawy, H. A. E. D. Bastawissi, P. Paramasivan, *et al.*, "Emission analysis on compression ignition engine fueled with lower concentrations of Pitheclobium dulce biodiesel-diesel blends," *Heat Transfer—Asian Research*, vol. 48, pp. 254-269, 2019.
- [10] M. Elkelawy, S. E.-d. H. Etaiw, H. A.-E. Bastawissi, H. Marie, A. Elbanna, H. Panchal, *et al.*, "Study of diesel-biodiesel blends combustion and emission characteristics in a CI engine by adding



- nanoparticles of Mn (II) supramolecular complex," *Atmospheric Pollution Research*, vol. 11, pp. 117-128, 2020/01/01/ 2020.
- [11] H. A. E. Bastawissi, M. Elkelawy, H. Panchal, and K. Kumar Sadasivuni, "Optimization of the multi-carburant dose as an energy source for the application of the HCCI engine," *Fuel*, vol. 253, pp. 15-24, 2019/10/01/ 2019.
  - [12] E. El Shenawy, M. Elkelawy, H. A.-E. Bastawissi, H. Panchal, and M. M. J. F. Shams, "Comparative study of the combustion, performance, and emission characteristics of a direct injection diesel engine with a partially premixed lean charge compression ignition diesel engines," vol. 249, pp. 277-285, 2019.
  - [13] M. M. El-Sheekh, M. Y. Bedaiwy, A. A. El-Nagar, M. Elkelawy, and H. Alm-Eldin Bastawissi, "Ethanol biofuel production and characteristics optimization from wheat straw hydrolysate: Performance and emission study of DI-diesel engine fueled with diesel/biodiesel/ethanol blends," *Renewable Energy*, vol. 191, pp. 591-607, 2022/05/01/ 2022.
  - [14] M. Elkelawy, E. A. El Shenawy, S. A. Mohamed, M. M. Elarabi, and H. A.-E. Bastawissi, "Impacts of using EGR and different DI-fuels on RCCI engine emissions, performance, and combustion characteristics," *Energy Conversion and Management: X*, vol. 15, p. 100236, 2022/08/01/ 2022.
  - [15] M. Elkelawy, H. Bastawissi, S. Chandra Sekar, K. Karuppasamy, N. Vedaraman, K. Sathiyamoorthy, *et al.*, "Numerical and experimental investigation of ethyl alcohol as oxygenator on the combustion, performance, and emission characteristics of diesel/cotton seed oil blends in homogenous charge compression ignition engine," 0148-7191, 2018.
  - [16] A. M. Elbanna, C. Xiaobei, Y. Can, M. Elkelawy, and H. A.-E. Bastawissi, "A comparative study for the effect of different premixed charge ratios with conventional diesel engines on the performance, emissions, and vibrations of the engine block," *Environmental Science and Pollution Research*, 2022/09/17 2022.
  - [17] H. A. E. Bastawissi, M. Elkelawy, H. Panchal, and K. K. J. F. Sadasivuni, "Optimization of the multi-carburant dose as an energy source for the application of the HCCI engine," vol. 253, pp. 15-24, 2019.
  - [18] M. Elkelawy, H. A.-E. Bastawissi, E. El Shenawy, M. Taha, H. Panchal, K. K. J. E. C. Sadasivuni, *et al.*, "Study of performance, combustion, and emissions parameters of DI-diesel engine fueled with algae biodiesel/diesel/n-pentane blends," vol. 10, p. 100058, 2021.
  - [19] M. Elkelawy, A. Kamel, A. Abou-elyazied, and S. M. El-malla, "Experimental investigation of the effects of using biofuel blends with conventional diesel on the performance, combustion, and emission characteristics of an industrial burner," *Egyptian Sugar Journal*, vol. 19, pp. 44-59, 2022.
  - [20] A. M. Elbanna, X. Cheng, C. Yang, M. Elkelawy, and H. A. Elden, "Knock Recognition System in a PCCI Engine Powered by Diesel," *Highlights in Science, Engineering and Technology*, vol. 15, pp. 94-101, 11/26 2022.
  - [21] M. Elkelawy, H. Alm Eldin Mohamad, M. Samadony, A. M. Elbanna, and A. M. S. M. Safwat, "Effect of Battery Charging Rates for Electric Hybrid Vehicle on Fuel consumption and emissions behaviors in different road conditions: a comparative Study with Conventional Car," *Journal of Engineering Research*, vol. 6, pp. 142-154, 2022.
  - [22] M. Elkelawy, H. A. E. Bastawissi, E. S. A. El-Shenawy, H. Panchal, K. Sadasivuni, D. Ponnammam, *et al.*, "Experimental investigations on spray flames and emissions analysis of diesel and diesel/biodiesel blends for combustion in oxy-fuel burner," vol. 14, p. e2375, 2019.
  - [23] I. Veza, M. F. M. Said, Z. A. Latiff, M. F. Hasan, R. I. A. Jalal, and N. M. I. N. Ibrahim, "Simulation of predictive kinetic combustion of single cylinder HCCI engine," *AIP Conference Proceedings*, vol. 2059, p. 020017, 2019.
  - [24] M. Q. Rusli, M. F. Muhammad Said, A. M. Sulaiman, M. F. Roslan, I. Veza, M. R. Mohd Perang, *et al.*, "Performance and Emission Measurement of a Single Cylinder Diesel Engine Fueled with Palm Oil Biodiesel Fuel Blends," *IOP Conference Series: Materials Science and Engineering*, vol. 1068, p. 012020, 2021/03/01 2021.
  - [25] M. Elkelawy, H. A.-E. Bastawissi, E. El Shenawy, M. M. Shams, H. Panchal, K. K. Sadasivuni, *et al.*, "Influence of lean premixed ratio of PCCI-DI engine fueled by diesel/biodiesel blends on combustion, performance, and emission attributes; a comparison study," vol. 10, p. 100066, 2021.
  - [26] M. Elkelawy, H. Alm Eldin Mohamad, E. Abd elhamid, and M. A. M. El-Gamal, "A Critical Review of the Performance, Combustion, and Emissions Characteristics of PCCI Engine Controlled by Injection Strategy and Fuel Properties," *Journal of Engineering Research*, vol. 6, pp. 96-110, 2022.
  - [27] M. Elkelawy, H. Alm Eldin Mohamad, A. K. Abdel-Rahman, A. Abou Elyazied, and S. Mostafa El malla, "Biodiesel as an Alternative Fuel in Terms of Production, Emission, Combustion Characteristics for Industrial Burners: a Review," *Journal of Engineering Research*, vol. 6, pp. 45-52, 2022.
  - [28] J.-z. Yu, Z. Yu-Sheng, M. Elkelawy, and Q. Kui, "Spray and combustion characteristics of HCCI engine using DME/diesel blended fuel by port-injection," SAE Technical Paper 0148-7191, 2010.
  - [29] M. Elkelawy, E. A. El Shenawy, S. A. Mohamed, M. M. Elarabi, and H. Alm-Eldin Bastawissi, "Impacts of EGR on RCCI engines management: A comprehensive review," *Energy Conversion and Management: X*, vol. 14, p. 100216, 2022/05/01/ 2022.
  - [30] M. Elkelawy, E. A. El Shenawy, H. Alm-Eldin Bastawissi, M. M. Shams, and H. Panchal, "A comprehensive review on the effects of diesel/biofuel blends with nanofluid additives on compression ignition engine by response surface methodology," *Energy Conversion and Management: X*, vol. 14, p. 100177, 2022/05/01/ 2022.
  - [31] A. Katijian, M. F. Abdul Latif, Q. F. Zahmani, S. Zaman, K. Abdul Kadir, and I. Veza, "An Experimental Study for Emission of Four Stroke Carbureted and Fuel Injection Motorcycle Engine," *Journal of Advanced Research in Fluid Mechanics and Thermal Sciences*, vol. 62, pp. 256-264, 12/23 2020.
  - [32] M. F. Roslan, I. Veza, and M. F. M. Said, "Predictive simulation of single cylinder n-butanol HCCI engine," *IOP Conference Series: Materials Science and Engineering*, vol. 884, p. 012099, 2020/07/01 2020.
  - [33] S. S. Kumar, K. Rajan, V. Mohanavel, M. Ravichandran, P. Rajendran, A. Rashedi, *et al.*, "Combustion, Performance, and Emission Behaviors of Biodiesel Fueled Diesel Engine with the Impact of Alumina Nanoparticle as an Additive," vol. 13, p. 12103, 2021.
  - [34] J. Chandran, K. Manikandan, R. Ganesh, and S. J. I. J. o. A. E. Baskar, "Effect of nano-material on the performance patterns of waste cooking biodiesel fuelled diesel engine," vol. 43, pp. 2226-2230, 2021.
  - [35] S. Ganesan, D. Munuswamy, P. Appavu, and T. J. J. o. O. P. R. Arunkumar, "Effect of EGR & nanoparticles on performance and emission characteristics of a diesel engine fuelled with palm biodiesel and diesel blends," vol. 31, pp. 130-137, 2019.
  - [36] D. Rangabashiam, A. J. E. S. Rameshbabu, Part A: Recovery, Utilization,, and E. Effects, "Emission, performance, and combustion study on nanoparticle-biodiesel fueled diesel engine," pp. 1-12, 2019.
  - [37] M. Gad, B. M. Kamel, and I. A. J. F. Badruddin, "Improving the diesel engine performance, emissions and combustion characteristics using biodiesel with carbon nanomaterials," vol. 288, p. 119665, 2021.
  - [38] M. Elkelawy, Z. Yu-Sheng, A. E.-D. Hagar, and J.-z. Yu, "Challenging and Future of Homogeneous Charge Compression Ignition Engines; an Advanced and Novel Concepts Review," *Journal of Power and Energy Systems*, vol. 2, pp. 1108-1119, 2008.
  - [39] Y. Devarajan, B. Nagappan, and G. Subbiah, "A comprehensive study on emission and performance characteristics of a diesel engine fueled with nanoparticle-blended biodiesel," *Environmental Science and Pollution Research*, vol. 26, pp. 10662-10672, 2019.
  - [40] M. E. M. Soudagar, M. Mujtaba, M. R. Safaei, A. Afzal, W. Ahmed, N. Banapurmath, *et al.*, "Effect of Sr@ ZnO nanoparticles and Ricinus communis biodiesel-diesel fuel blends on modified CRDI diesel engine characteristics," *Energy*, vol. 215, p. 119094, 2021.
  - [41] A. T. Hoang, "Combustion behavior, performance and emission characteristics of diesel engine fuelled with biodiesel containing cerium oxide nanoparticles: A review," *Fuel Processing Technology*, vol. 218, p. 106840, 2021.
  - [42] M. Elkelawy, S. E.-d. H. Etaiw, M. I. Ayad, H. Marie, M. Dawood, H. Panchal, *et al.*, "An enhancement in the diesel engine performance, combustion, and emission attributes fueled by diesel-biodiesel and 3D silver thiocyanate nanoparticles additive

- fuel blends," *Journal of the Taiwan Institute of Chemical Engineers*, vol. 124, pp. 369-380, 2021.
- [43] F. Hussain, M. E. M. Soudagar, A. Afzal, M. Mujtaba, I. R. Fattah, B. Naik, *et al.*, "Enhancement in combustion, performance, and emission characteristics of a diesel engine fueled with Ce-ZnO nanoparticle additive added to soybean biodiesel blends," *Energies*, vol. 13, p. 4578, 2020.
- [44] M. Elkelawy, S. E.-d. H. Etaiw, H. A.-E. Bastawissi, M. I. Ayad, A. M. Radwan, and M. M. J. E. Dawood, "Diesel/biodiesel/silver thiocyanate nanoparticles/hydrogen peroxide blends as new fuel for enhancement of performance, combustion, and Emission characteristics of a diesel engine," vol. 216, p. 119284, 2021.
- [45] M. Elkelawy, S. E.-d. H. Etaiw, H. A.-E. Bastawissi, H. Marie, A. Elbanna, H. Panchal, *et al.*, "Study of diesel-biodiesel blends combustion and emission characteristics in a CI engine by adding nanoparticles of Mn (II) supramolecular complex," vol. 11, pp. 117-128, 2020.
- [46] Ü. Ağbulut, S. Sarıdemir, U. Rajak, F. Polat, A. Afzal, and T. N. J. E. Verma, "Effects of high-dosage copper oxide nanoparticles addition in diesel fuel on engine characteristics," vol. 229, p. 120611, 2021.
- [47] K. Kalaimurugan, S. Karthikeyan, M. Periyasamy, and G. J. M. T. P. Mahendran, "Experimental investigations on the performance characteristics of CI engine fuelled with cerium oxide nanoparticle added biodiesel-diesel blends," vol. 33, pp. 2882-2885, 2020.
- [48] I. Örs, S. Sarıkoç, A. Atabani, S. Ünalın, and S. J. F. Akansu, "The effects on performance, combustion and emission characteristics of DIC engine fuelled with TiO<sub>2</sub> nanoparticles addition in diesel/biodiesel/n-butanol blends," vol. 234, pp. 177-188, 2018.
- [49] A. Yaşar, A. Keskin, Ş. Yıldızhan, and E. J. F. Uludamar, "Emission and vibration analysis of diesel engine fuelled diesel fuel containing metallic based nanoparticles," vol. 239, pp. 1224-1230, 2019.
- [50] S. Hoseini, G. Najafi, B. Ghobadian, M. Ebadi, R. Mamat, and T. J. R. e. Yusaf, "Biodiesels from three feedstock: The effect of graphene oxide (GO) nanoparticles diesel engine parameters fuelled with biodiesel," vol. 145, pp. 190-201, 2020.
- [51] Q. Wu, X. Xie, Y. Wang, and T. J. A. E. Roskilly, "Effect of carbon coated aluminum nanoparticles as additive to biodiesel-diesel blends on performance and emission characteristics of diesel engine," vol. 221, pp. 597-604, 2018.
- [52] M. Elkelawy, S. E.-d. H. Etaiw, H. A.-E. Bastawissi, H. Marie, A. M. Radwan, M. M. Dawood, *et al.*, "WCO biodiesel production by heterogeneous catalyst and using cadmium (II)-based supramolecular coordination polymer additives to improve diesel/biodiesel fueled engine performance and emissions," *Journal of Thermal Analysis and Calorimetry*, vol. 147, pp. 6375-6391, 2022/06/01 2022.
- [53] A. Mohammed Elbanna, C. Xiaobei, Y. Can, M. Elkelawy, H. Alm-Eldin Bastawissi, and H. Panchal, "Fuel reactivity controlled compression ignition engine and potential strategies to extend the engine operating range: A comprehensive review," *Energy Conversion and Management: X*, vol. 13, p. 100133, 2022/01/01/ 2022.
- [54] M. ElKelawy, H. A.-E. Bastawissi, E.-S. A. El-Shenawy, H. Panchal, K. Sadashivuni, D. Ponnammam, *et al.*, "Experimental investigations on spray flames and emissions analysis of diesel and diesel/biodiesel blends for combustion in oxy-fuel burner," *Asia-Pacific Journal of Chemical Engineering*, vol. 14, p. e2375, 2019.
- [55] M. Elkelawy, S. E.-d. H. Etaiw, H. Alm-Eldin Bastawissi, M. I. Ayad, A. M. Radwan, and M. M. Dawood, "Diesel/ biodiesel /silver thiocyanate nanoparticles/hydrogen peroxide blends as new fuel for enhancement of performance, combustion, and Emission characteristics of a diesel engine," *Energy*, vol. 216, p. 119284, 2021/02/01/ 2021.
- [56] S. El-din H. Etaiw, M. Elkelawy, I. Elziny, M. Taha, I. Veza, and H. Alm-Eldin Bastawissi, "Effect of nanocomposite SCP1 additive to waste cooking oil biodiesel as fuel enhancer on diesel engine performance and emission characteristics," *Sustainable Energy Technologies and Assessments*, vol. 52, p. 102291, 2022/08/01/ 2022.
- [57] M. Elkelawy, H. Alm Eldin Mohamad, M. Samadony, A. M. Elbanna, and A. M. S. M. Safwat, "A Comparative Study on Developing the Hybrid-Electric Vehicle Systems and its Future Expectation over the Conventional Engines Cars," *Journal of Engineering Research*, vol. 6, pp. 21-34, 2022.
- [58] J. C. J. I. Mallinson, Harcourt Brace Jovanovich, San Diego, "The Foundations of Magnetic Recording Academic Press," 1987.
- [59] S. Ito, P. Liska, P. Comte, R. Charvet, P. Péchy, U. Bach, *et al.*, "Control of dark current in photoelectrochemical (TiO<sub>2</sub>/I<sup>-</sup>/I<sup>3-</sup>) and dye-sensitized solar cells," pp. 4351-4353, 2005.
- [60] R. V. Kumar, Y. Diamant, and A. J. C. o. M. Gedanken, "Sonochemical synthesis and characterization of nanometer-size transition metal oxides from metal acetates," vol. 12, pp. 2301-2305, 2000.
- [61] A. A. Eliseev, A. V. Lukashin, A. A. Vertegel, L. I. Heifets, A. I. Zhironov, and Y. D. J. M. R. I. Tretyakov, "Complexes of Cu (II) with polyvinyl alcohol as precursors for the preparation of CuO/SiO<sub>2</sub> nanocomposites," vol. 3, pp. 308-312, 2000.
- [62] J. Xu, W. Ji, Z. Shen, S. Tang, X. Ye, D. Jia, *et al.*, "Preparation and characterization of CuO nanocrystals," vol. 147, pp. 516-519, 1999.
- [63] K. Borgohain, J. B. Singh, M. R. Rao, T. Shripathi, and S. J. P. R. B. Mahamuni, "Quantum size effects in CuO nanoparticles," vol. 61, p. 11093, 2000.
- [64] S. Nakao, M. Ikeyama, T. Mizota, P. Jin, M. Tazawa, Y. Miyagawa, *et al.*, "Attempts of the formation of metal oxide nanoparticles by co-implantation of metal and oxygen ions," pp. 153-158, 2000.